

Subtle dimensions of climate change have strong
demographic effects on a cactus population in
extinction debt

Kevin Czachura and Tom E.X. Miller*

Program in Ecology and Evolutionary Biology, Department of
BioSciences, Rice University, Houston, TX USA

*Corresponding author: tom.miller@rice.edu (1-713-348-4218)

Abstract

- 1 1. The effects of climate change on population viability reflect the net influ-
2 ence of potentially diverse responses of individual-level demographic pro-
3 cesses (growth, survival, regeneration) to multiple components of climate.
4 Articulating climate-demography connections can facilitate forecasts of re-
5 sponses to future climate change as well as back-casts that may reveal how
6 populations responded to historical climate change.
- 7 2. We studied climate-demography relationships in the cactus *Cyclindriopun-*
8 *tia imbricata*; previous work indicated that our focal population has high
9 abundance but a negative population growth rate, where deaths exceed
10 births, suggesting that it persists under extinction debt. We parameter-
11 ized a climate-dependent integral projection model with data from a 14-year
12 field study, then back-casted expected population growth rates since 1900
13 to test the hypothesis that recent climate change has driven this population
14 into extinction debt.
- 15 3. We found clear patterns of climate change in our central New Mexico study
16 region but, contrary to our hypothesis, *C. imbricata* has most likely bene-
17 fitted from recent climate change and is on track to reach replacement-level
18 population growth within 38 years, or sooner if climate change accelerates.
19 Furthermore, the strongest feature of climate change (a trend toward years
20 that are overall warmer and drier, captured by the first principal component
21 of inter-annual variation) was not the main driver of population responses.
22 Instead, temporal trends in population growth were dominated by more sub-

23 tle, seasonal climatic factors with relatively weak signals of recent change
24 (wetter and milder cool seasons, captured by the second and third principal
25 components).

26 4. *Synthesis*. Our results highlight the challenges of forecasting population dy-
27 namics under climate change, since the most apparent features of climate
28 change may not be the most important drivers of ecological responses. Envi-
29 ronmentally explicit demographic models can help meet this challenge, but
30 they must consider the magnitudes of different aspects of climate change
31 alongside the magnitudes of demographic responses to those changes.

32 **Keywords**

33 Cactaceae; Climate change; Demography; Extinction debt; Integral Projection
34 Model; Long-term ecological research

Introduction

Understanding abiotic drivers of distribution and abundance is a foundational objective of ecology and takes on urgency in the context of ongoing global climate change. The study of population dynamics is particularly well suited to identifying climate drivers, and this may facilitate forecasting responses to future climate change or back-casting responses to historical climate trends. Climate drivers may be inferred from temporal fluctuations in population size or individual demographic performance; in either case, long-term data are essential for teasing apart the roles of particular climatic factors from other sources of inter-annual variability.

Population extinction debt is likely to increase in frequency as a fingerprint of global change, including climate change (Dullinger *et al.*, 2012; Urban, 2015). Extinction debt is a form of transient dynamics whereby populations persist despite having population growth rates that fall below replacement level ($\lambda = 1$), suggesting a long-term trajectory toward local extinction but with long time lags (Hastings *et al.*, 2018; Kuussaari *et al.*, 2009). This may be more likely for species with life cycles that are slow relative to environmental change (Vellend *et al.*, 2006). While extinction debt is often studied through species richness patterns at the community level, there is recent emphasis on the underlying single-species dynamics whereby populations transition from positive to negative growth rates (Lehtilä *et al.*, 2016; Hylander & Ehrlén, 2013). In the absence of significant migration (which can maintain populations in sink habitats), population extinction debt is indicative of environmental change, since transient persistence suggests that the environment was favorable for population growth at some time in the past. However, while evidence for extinction debt is growing, the mechanisms that

59 cause populations to tip from positive to negative growth rates are rarely known,
60 and this information may be critical for effective conservation planning (Hylander
61 & Ehrlén, 2013).

62 Structured population models built from individual-level demographic rates
63 provide a powerful framework for studying drivers of extinction debt (Lehtilä *et al.*,
64 2016) and environment-dependent population dynamics more generally (Ehrlén &
65 Morris, 2015). These methods derive predictions for population growth and via-
66 bility from a suite of statistical models fitted to individual-level vital rates. By
67 incorporating climatic factors as statistical covariates, previous studies have iden-
68 tified climatic limits of population viability and forecasted responses to particular
69 types of climate change (e.g., Adler *et al.* 2013; Maschinski *et al.* 2006; Jenouvrier
70 *et al.* 2014). Additionally, articulating the connections between environment and
71 demography can allow for ‘back-casting’ population dynamics into historical envi-
72 ronmental regimes (Smith *et al.*, 2005), which may provide insight regarding when
73 and why populations fell into extinction debt.

74 Despite the potential of demographic methods to reveal climate drivers of
75 population dynamics, there are several challenges in scaling up from individual-
76 level data to population responses to environmental change. Climate change is a
77 multi-dimensional process that may involve shifts in the means, variances, extreme
78 events, and seasonal distributions of multiple variables related to temperature and
79 precipitation (IPCC, 2013). Many studies of climate-demography relationships
80 focus on single climate variables that are known to be a dominant component of
81 climate change and / or known to have a strong influence on the focal species (e.g.,
82 Van de Pol *et al.* 2010; Iler *et al.* 2019; Jenouvrier *et al.* 2009). However, for many
83 species, it is not always apparent *a priori* which dimensions of climate are most

important, and this poses challenges for predicting population responses to climate change. Previous studies have shown that different components of climate change may have independent effects on different aspects of demography or physiology, such as distinct effects of climate means versus extremes (Buckley & Kingsolver, 2012; Frederiksen *et al.*, 2008; Van de Pol *et al.*, 2010; Lynch *et al.*, 2014). Furthermore, different life stages (e.g., young vs old) and different vital rate processes (e.g., growth, survival, reproduction) may differ in the magnitude and even direction of their responses to single climate drivers (Doak & Morris, 2010; Dybala *et al.*, 2013; Morrison & Hik, 2007; Tenhumberg *et al.*, 2018), and single life stages or vital rates may be affected by multiple drivers (Dalglish *et al.*, 2011; Williams *et al.*, 2015; Frederiksen *et al.*, 2008; Sletvold *et al.*, 2013). Ultimately, the influence of climate on population growth depends on the sensitivities of vital rates to climate drivers and the sensitivities of λ to the vital rates, integrated across the life cycle (McLean *et al.*, 2016; Ådahl *et al.*, 2006). These complications, common to environmentally explicit demographic studies (Ehrlén *et al.*, 2016), highlight the value of leveraging long-term data to gain resolution of climate drivers and the importance of accounting for demographic complexity across the life cycle.

We used long-term demographic data to study climate-dependent population dynamics of a long-lived Chihuahuan desert cactus persisting under extinction debt. Our previous work with the tree cholla cactus (*Cylindriopuntia imbricata* Haw. D.C.) (Cactaceae) indicated, with >95% certainty, that our focal population in the northern Chihuahuan Desert (New Mexico, USA) is in decline (stochastic population growth rate $\lambda_S < 1$) despite current densities that are reasonably high (Ohm & Miller, 2014; Miller *et al.*, 2009; Elder & Miller, 2016). Our study region has experienced strong climatic fluctuations over the past century, including several

109 decadal-scale droughts interrupted by relatively wet periods (Peters *et al.*, 2015).
110 Recent and projected climate change in our study region includes increases in
111 temperature and shifts in the seasonal timing of precipitation (Petrie *et al.*, 2014;
112 Cook & Seager, 2013; Cook *et al.*, 2015).

113 Previous studies have generated heterogeneous results regarding cactus re-
114 sponses to climate drivers. While cacti are famous for adaptations to arid environ-
115 ments (e.g., CAM photosynthesis, photosynthetic stems) and have been observed
116 to increase in abundance during drought (Cook, 1942), several studies suggest that
117 cactus growth and regeneration may be limited by rainfall (Parker, 1993; Drezner
118 & Balling, 2002; Winkler *et al.*, 2018). Furthermore, there may be contrasting
119 responses to precipitation that falls during the cool and wet seasons (Drezner,
120 2003; Bowers, 2005; Hultine *et al.*, 2018). Other studies suggest key roles of tem-
121 perature, and especially winter temperature minima, as a determinant of cactus
122 mortality (Kinraide, 1978; Flores & Yeaton, 2003) and reproduction (Bustamante
123 & Búrquez, 2008). No previous studies have attempted to integrate the poten-
124 tially diverse demographic responses of cacti to seasonal climatic factors within a
125 demographic modeling framework, which is essential for understanding how these
126 pieces fit together to determine overall population responses to climatic variability.
127 Given the important role cacti and other CAM plants in drylands worldwide, there
128 is a need to better understand their responses to past and future climate change
129 (Reyes-García & Andrade, 2009; Yu *et al.*, 2019).

130 This study was designed to understand how historical climate patterns affected
131 population viability in *C. imbricata* and to test the hypothesis that recent climate
132 change has driven this population into extinction debt; this hypothesis predicts
133 that historical climatic conditions were more favorable for population growth than

134 present-day conditions. We also sought to identify which aspects of climate are
135 changing most strongly, and then ask whether the strongest features of climate
136 change are the most important determinants of population responses. Our specific
137 aims were to:

- 138 • Characterize climate variation and change in our northern Chihuahuan desert
139 study region over the past century
- 140 • Quantify cactus vital rate responses to inter-annual climate variation during
141 the demographic study period (2004–2017)
- 142 • Back-cast climate-dependent population growth to determine whether the
143 past century included periods that were favorable for population growth
- 144 • Identify which aspects of climate (cool and warm season temperature and
145 precipitation) are changing most strongly, and which demographic responses
146 to climate (growth, survival, reproduction) most strongly determine tempo-
147 ral trends in population growth

148 **Materials and methods**

149 **Study site and demographic data collection**

150 Tree cholla cactus is widely distributed throughout desert and grassland habitats
151 of the southwest U.S. and northern Mexico. These long-lived plants (40-plus years)
152 grow through the production and elongation of cylindrical stem segments. These
153 vegetative structures as well as flowerbuds are initiated in late spring. Flower-
154 ing occurs in early summer and stem segment elongation takes place during the

155 remainder of the growing season. For climate analyses, we divide the calendar
156 year into warm-season months (May through September), when stem elongation,
157 flowering, and seed production occur, and cool-season months (October through
158 April).

159 This study was conducted at the Sevilleta National Wildlife Refuge (SNWR), a
160 Long-Term Ecological Research site (SEV-LTER) in central New Mexico and near
161 the center of this species' geographic distribution. Our study population occurs in
162 the Los Piños mountains at an elevation of 1790 m. Tree cholla are a dominant
163 component of the vegetation in this area (0.1 m^{-2} : Miller *et al.* 2009), along with
164 oaks, yucca, Piñon pine, and the grasses *Bouteloua gracilis* and *B. eriopoda*.

165 The present study relies on long-term (2004–2017) demographic data on individual-
166 level measures of growth, survival, and reproduction recorded from tagged plants
167 in the Los Piños population that were censused in late May each year. This was
168 a pre-breeding census that corresponds to the initiation of vegetative and repro-
169 ductive structures (Fig. C1). We treat May 1 as the start of the transition year
170 (coincident with the start of the warm-season months). There were a total of 1172
171 unique individuals in the data set and 7442 transition-year observations from 4–8
172 plots or spatial blocks depending on the year. Full details of the study design and
173 data collection are given elsewhere (Miller *et al.*, 2009; Ohm & Miller, 2014; Elderd
174 & Miller, 2016).

175 Climate data

176 Our goal was to connect inter-annual variation in demography to corresponding
177 variation in temperature and precipitation. SEV-LTER collects climate data from

178 a network of meteorological stations throughout SNWR, with the oldest records
179 coming from the late 1980s. While the SEV-LTER climate data cover years of
180 our demographic data collection, our intention was to back-cast demographic per-
181 formance farther back into the 20th century. We therefore gathered climate data
182 from ClimateWNA v5.60 (Wang *et al.*, 2016), a software package that uses PRISM
183 (Daly *et al.*, 2008) and WorldClim (Hijmans *et al.*, 2005) data to calculate down-
184 scaled data for western North America based on location and elevation, going as
185 far back as 1900. By relying on downscaled, interpolated climate data instead of
186 direct observations from meteorological stations we are trading off local resolution
187 in favor of more historical years of data. We quantified this loss of resolution by
188 comparing predictions from ClimateWNA to SEV-LTER data for years that they
189 over-lapped, using the SEV-LTER meteorological station that was nearest our
190 study population (Appendix A). We found that the two data sets were highly cor-
191 related (Table A1, Figure A1), which bolstered our confidence that ClimateWNA
192 provided locally accurate climate data for both the demographic observation pe-
193 riod as well as historical years that preceded our study.

194 We derived seasonal estimates (warm- and cool-season) of total precipitation
195 and mean, minimum, and maximum temperature from monthly climate data, for
196 a total of eight variables. Months were aligned to correspond to demographic
197 transition years rather than calendar years, which means the cool-season climate
198 for a transition year beginning in May of year t spans October of year t through
199 April of year $t + 1$ (Fig. C1).

200 To reduce the dimensionality of the climate data, we conducted Principal Com-
201 ponents Analysis (PCA) on the eight climate variables for the years 1900-2017,
202 with climate values scaled to unit variance. We estimated the variance in the raw

climate data explained by each PC and the variable loadings, which give the correlations between original variables and PC values. PCA allowed us to rank the magnitudes of multiple aspects of climate variation and change by examining how warm- and cool-season variables loaded onto the ranked PC axes.

Statistical estimation of climate-dependence

We built generalized linear mixed models (GLMM) in a hierarchical Bayesian framework to connect inter-annual demographic variability to climate drivers, as captured by three PCs that collectively explained 73.3% of the inter-annual variation in seasonal climate values (Results). The choice of three PCs was based on results of parallel analysis (Fig. A2), a statistical method for determining how many components to retain (Franklin *et al.*, 1995). Climate-dependence was limited to the four demographic vital rates for which we had long-term data: survival, growth (change in size), reproductive status (vegetative or flowering), and fertility of flowering plants (number of flower buds produced). For each of these vital rates, we fit a statical model that included fixed effects of size, climate, size*climate interaction, and a quadratic term for climate to account for possible non-monotonic effects. “Climate” in these models was each of the three PCs, so there were a total of 10 candidate variables for each vital rate model (Appendix B). We used stochastic variable selection in a Bayesian framework to reduce model complexity, dropping coefficients that were effectively zero with $\geq 90\%$ certainty. All models additionally included random intercepts for spatial (plot) and temporal (year) heterogeneity. The year random-effect can be interpreted as inter-annual variability in demography that cannot be explained by the climate PCs. Full details for the

226 statistical models are provided in Appendix B.

227 Survival and growth from year $t - 1$ to t were dependent on size in year $t - 1$,
228 and the climate covariate corresponded to the climate year $t - 1$ to t . Reproductive
229 status and fertility in year t were dependent on size in year t and on climate from
230 $t - 1$ to t . This timing of size and climate effects was intended to match processes
231 in the population model (see life cycle diagram in Fig. C1). We did not quantify
232 climate-dependence in seedling recruitment. While we searched plots each year
233 and added newly detected plants to the census, we could not confidently assign a
234 birth year to these new additions (seedlings require several years of growth before
235 they are consistently detectable in our census) so we do not know the climatic
236 conditions under which they recruited.

237 **Demographic modeling**

238 We used the statistical models for vital rate responses to build a stochastic, size-
239 structured integral projection model that incorporated climate dependence. De-
240 tails of IPM construction and analysis are provided in Appendix C; here we provide
241 a brief overview. We used the model to predict how the asymptotic population
242 growth rate (λ) responds to different components of climate variability and change,
243 and to identify the demographic processes underlying those responses. First, to
244 evaluate the consequences of different aspects of climate, we quantified the rela-
245 tionship between λ and each of the three principal components of climate variation,
246 holding the other two constant at their long-term means. Because we estimated
247 vital rates in a Bayesian framework, we were able to generate posterior distribu-
248 tions of λ that reflect the combined uncertainties of all the underlying vital rates.

249 Second, we used statistical relationships between climate drivers and vital rate
250 responses estimated during our 14-year field study to back-cast expected popu-
251 lation growth rates over the entire climatological record that we had available,
252 1900–2017. We used linear regression to test for temporal trends in λ over this
253 period. We incorporated two types of uncertainty into back-casted values of λ :
254 imperfect knowledge of the parameter values (“estimation error”) and year-to-year
255 fluctuations that were not related to climate (“process error”); the latter was es-
256 timated from the variances of random year effects. For the years of demographic
257 data collection (2004–2017), we could additionally quantify the deviations between
258 predicted λ based solely on climate and “observed” λ that reflects climate and non-
259 climate year effects (quotations indicate that these are the asymptotic predictions
260 given the vital rates observed in that year). We used a fixed-design Life Table
261 Response Experiment to decompose the total response of λ to climatic variation
262 into contributions from each of the climate PCs and each of the underlying vi-
263 tal rate responses. We found good qualitative correspondence between predicted
264 and observed size distributions (Fig. C2), which bolstered our confidence that the
265 model accurately described the dynamics of our focal population.

266 Finally, we estimated a time series for the stochastic population growth rate
267 (λ_S) over the period 1900–2017 using a moving window approach with a window
268 size of 10 years. While the deterministic growth rate for each year estimates the
269 long-run growth rate expected if the conditions of that year remained constant, the
270 stochastic growth rate integrated over a broader range of conditions, incorporating
271 year-to-year fluctuations and auto-correlation of climate variables.

Results

Climate trends

Three principal components cumulatively explained 73.3% of the inter-annual variation in climate (Figure 1A); we focus on these three PCs as climate drivers of demography. PC1, which explained 33.57% of variation, was dominated by inter-annual differences in temperature and precipitation, regardless of season, and the three components of temperature (mean, min, max) loaded similarly onto this component (Figure 1B). Over the last century, PC1 trends have fluctuated, with prolonged stretches of warm and dry years (the 1950s and early 2000s) and other periods of cool and wet years (early 1900s and 1970s-80s), though the overall temporal trend for PC1 is negative ($F_{1,114} = 21.72$, $P \leq 10^{-5}$). The decline per-year is nearly five times stronger since 1970 compared to the long-term average (Fig. 1C), suggesting an accelerating trajectory of warmer and drier years.

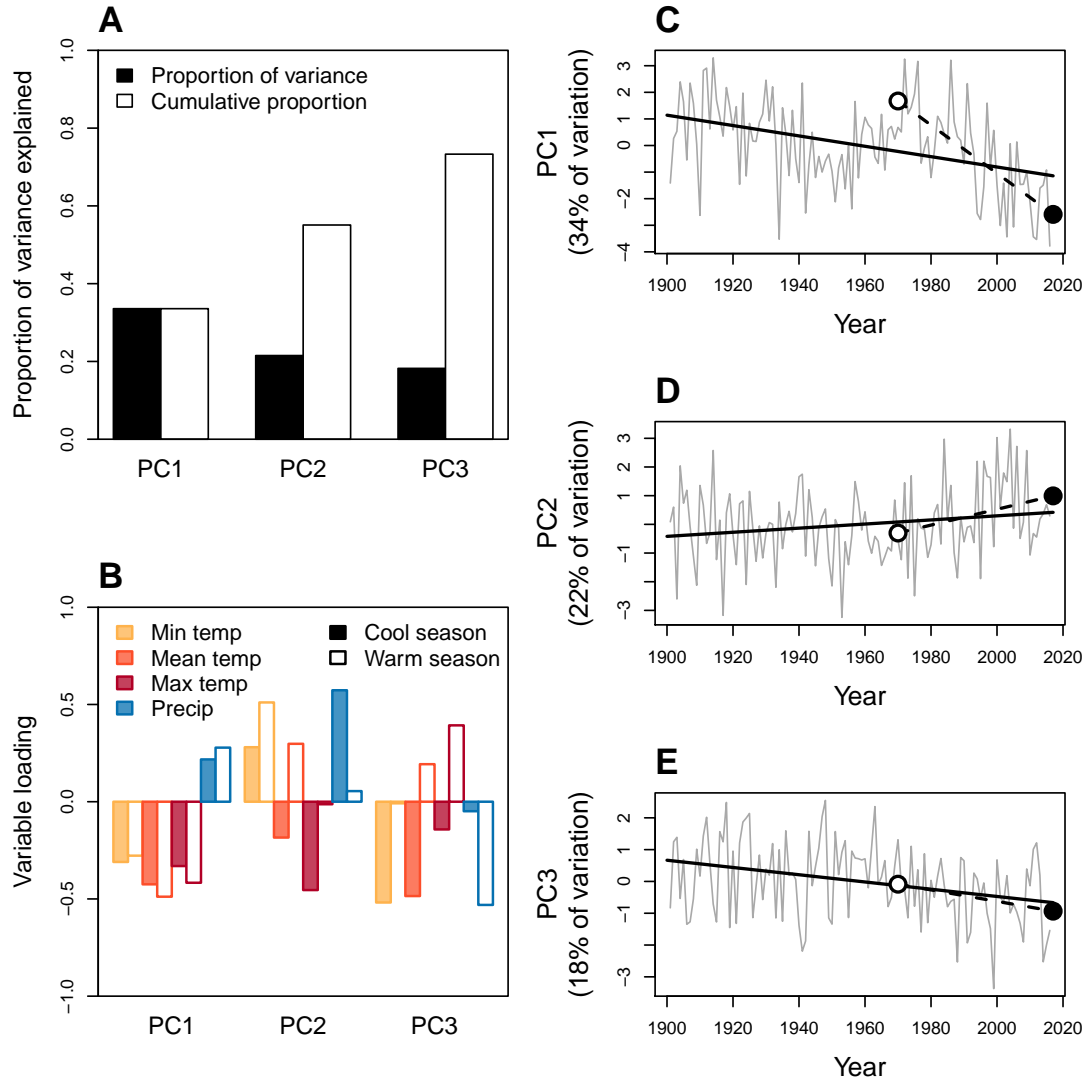


Figure 1: Principal components analysis (PCA) of inter-annual climate variability at SNWR, 1901–2017. **A**, Proportion and cumulative proportion of variation in seasonal temperatures (minimum, mean, maximum) and precipitation explained by the first three PCs. **B**, Loadings of seasonal climate variables onto PC1-3. Because climate data were standardized to mean zero and unit variance, loadings can be interpreted as the correlation between the climate variable and the PC. **C–E**, Time series of PC values, with regression lines showing long-term trends since 1901 (solid lines) or 1970 (dashed lines); open and filled points indicate the years 1970 and 2017, respectively, and correspond to the same shapes in Fig. 3

285 The second principal component explained 21.52% of climate variation (Figure
 286 1A) and was strongly driven by cool-season climate, especially precipitation, such
 287 that greater values corresponded to wetter winters with low temperature maxima
 288 and high temperature minima (Figure 1B). Warm-season temperatures also loaded
 289 positively onto this axis to a lesser degree (Figure 1B). PC2 has increased signifi-
 290 cantly significantly since 1900 ($F_{1,45} = 40.17$, $P \leq 10^{-7}$) and the change per-year
 291 is nearly four times stronger since 1970 (Figure 1D), indicating an accelerating
 292 trend of wetter cool seasons with moderate winter temperatures.

293 Lastly, PC3 explained 18.22% of climate variation (Figure 1A) and was corre-
 294 lated with a combination of warm- and cool-season climate variables. The strongest
 295 variable loadings on this principal component were minimum and mean tempera-
 296 tures in the cool season and warm-season precipitation. Temporal trends for PC3
 297 show weak declines since 1900 ($F_{1,114} = 12.77$, $P \leq 5.2 \times 10^{-4}$), correspdoning
 298 to milder winters with higher minimum and mean temperatures and wetter warm
 299 seasons; this trend has been slightly stronger since 1970 (Figure 1E).

300 **Vital rate responses to climate**

301 Demographic vital rates estimated from long-term data (survival, growth, repro-
 302 ductive status, and fertility of flowering plants) were least responsive to PC1,
 303 the dominant axis of climate variability and change, and more responsive to less
 304 variable climate dimensions. All of the vital rates were strongly, positively size-
 305 dependent but there was heterogeneity in the magnitude and sign of responses to
 306 different dimensions of climate variability. Figure 2 shows vital rate data and fit-
 307 ted statistical models (including size- and climate-dependence) following variable

308 selection procedures that eliminated coefficients that were weakly supported (Ta-
309 ble B1). There was very little support for coefficients of quadratic climate effects
310 (Table B1), indicating that responses to climate were monotonic over the range of
311 variation we observed.

312 For PC1, there was a weak reduction in survival probability (especially for
313 smaller plants; Fig. 2A) and a moderate reduction in flowering probability (espe-
314 cially for larger plants; Fig. 2G) at higher PC values, i.e., in cooler and wetter
315 years. Fertility of flowering plants was not responsive to PC1 variation (Fig. 2J)
316 and growth was not responsive to any of the climate PCs (Fig. 2D,E,F). There
317 were positive responses to PC2 in survival (Fig. 2B), flowering probability (Fig.
318 2H), and fertility of flowering plants (Fig. 2K), indicating that these vital rates
319 benefitted from years with wetter cool seasons. Responses to PC3 varied in sign,
320 with survival increasing with decreasing PC values (years with mild winter temper-
321 ature minima and wet summers) and reproductive rates increasing with increasing
322 PC values (years with low winter minima and dry summers) (Fig. 2C,I,L).

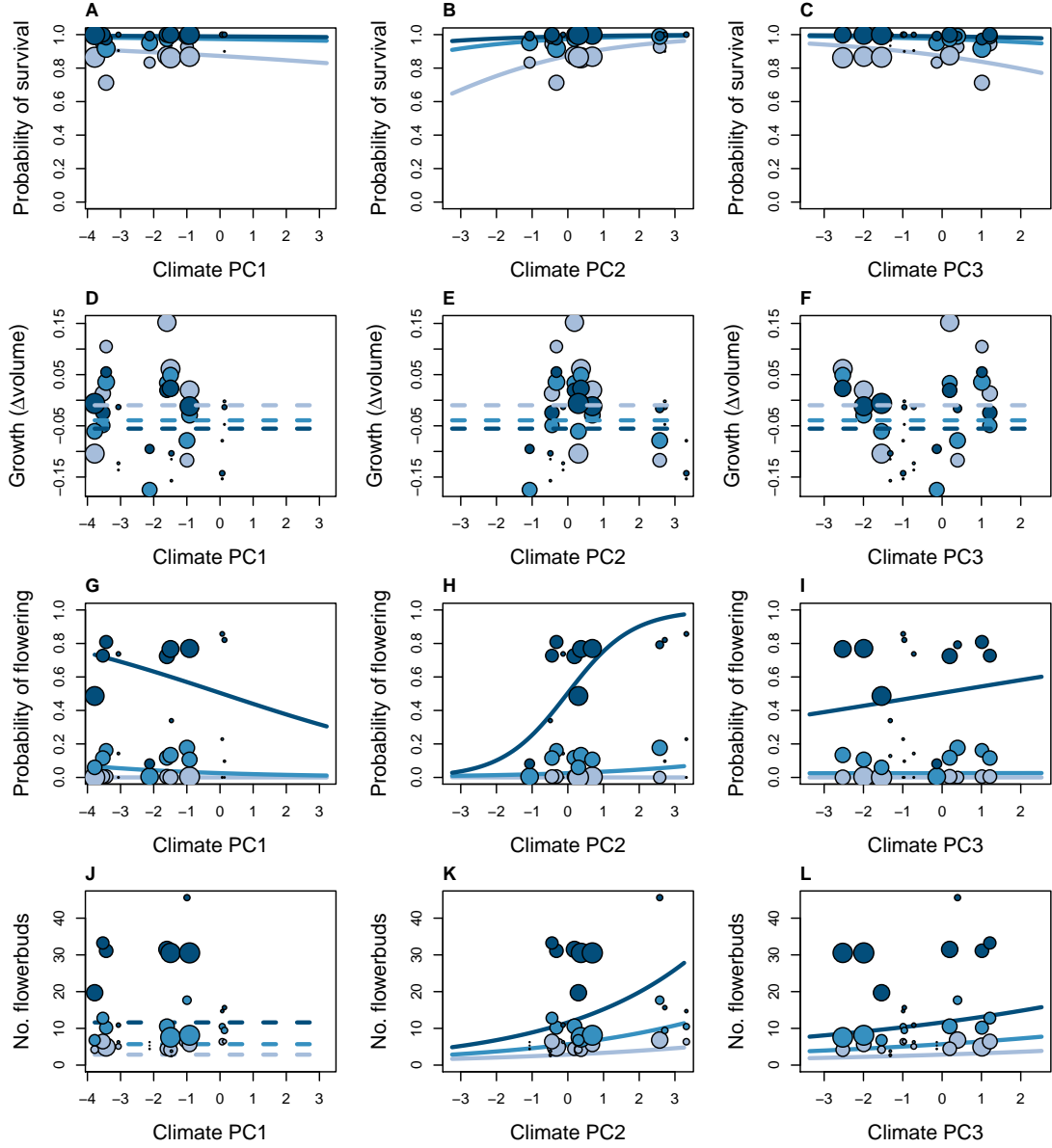


Figure 2: Climate- and size-dependent variation in survival (A-C), growth (D-F), flowering (G-I), and fertility of flowering plants (J-L) in relation to three principal components of seasonal climate variation (columns). For visualization only, the plant size distribution was discretized into three groups (small, medium, and large, corresponding to increasingly dark shading). Points show means for each size group in each year, where different years have unique PC values and point size is proportional to sample size for each size group in each year. Lines show fitted statistical models using posterior mean parameter values, with shading corresponding to size groups. Dashed lines indicate that the climate predictor was not statistically supported. Ranges of x -axes show the climate extrapolation that was required for back-casting.

Climate-dependent population growth

Integrating across vital rate responses, the population growth rate λ was predicted to increase with decreasing values of PC1 (hotter, drier years), holding other PCs fixed at their long-term average (Fig. 3A). Population growth was also predicted to increase with increasing values of PC2 (wetter cool seasons; Fig. 3B). Population growth was more sensitive to PC2 than PC1, such that the predicted change in λ from 1970 to 2017 was slightly greater for PC2 even though PC1 exhibited much greater change than PC2 over this period. Finally, greater values of PC3 (colder winters and drier summers) were predicted to cause declines in population growth, indicating that negative effects on cactus survival outweighed positive effects of PC3 on reproduction (Fig. 2). PC3 has changed relatively little since 1970 but this was associated with a change in λ of about half the magnitude to the response to relatively large change in PC1. Overall, recent climate change in each of the principal components, in isolation, has been in the direction that favors increased population growth (Fig. 1, 3). However, mean estimates for population growth rates were consistently below replacement level for all climate PC values, and the posterior probability densities rarely met or exceeded $\lambda = 1$.

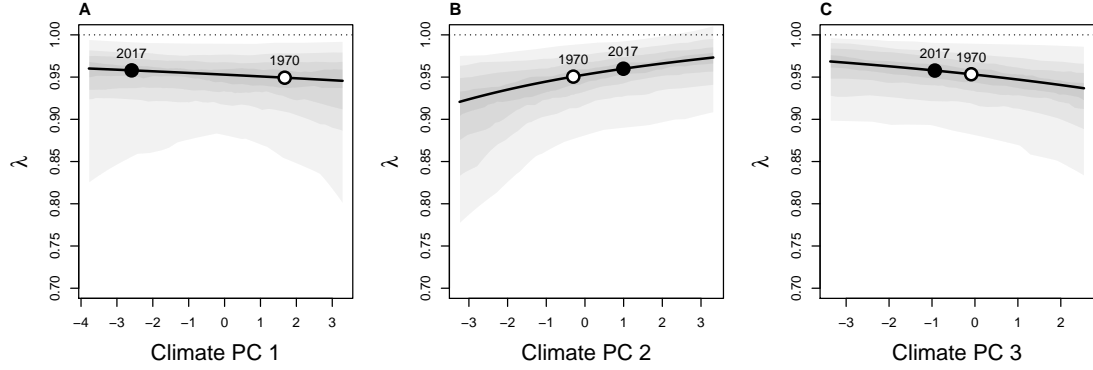


Figure 3: Predicted asymptotic population growth rate (λ) in response to three principal components of inter-annual climatic variation (A-C). For each panel, the indicated principal component is varying while the others are held at zero (the average value). Lines show the expected relationships based on posterior mean parameter values and shaded contours show the 25,50,75, and 95% credible intervals, representing uncertainty in demographic parameters. Points highlight the change the PC value (on the x -axis) between 1970 and 2017, based on the regression lines shown in Fig. 1, and the predicted corresponding change in λ (y -axis).

Back-casting population growth

Figure 4A shows the back-casted time series of λ accounting for inter-annual variation in all three PC components. For the the observation years (2004-2017) we incorporated additional sources of variability, estimated as statistical random effects, in year-specific estimates of λ (points in Fig. 4A). For these years, the three climate PCs explained 57% of the inter-annual variation in λ . Thus, even with relatively strong climate-demography associations (Fig. 2), there was substantial uncertainty in our back-casted estimates of λ due to process error, i.e., heterogeneity in vital rates across years that could not be attributed to the climate PCs. This uncertainty, combined with uncertainty arising from imperfect knowledge of

the underlying parameters, is shown in the shaded regions of Fig. Figure 4A.

Despite uncertainty in our back-cast, the results indicated that λ has likely remained below replacement levels for more than a century; there was no evidence that climate change drove this population into extinction debt. To the contrary, there was a positive temporal trend ($\frac{\Delta\lambda}{\Delta Year} > 0$), suggesting a trajectory of increasing population growth rates through time (Fig. 4B). There was wide uncertainty in the rate of change (corresponding to our imperfect ability to back-cast λ based on climate alone) but the posterior probability distribution indicated that it was 2.27 times more likely that λ has increased than decreased. Furthermore, the median rate of increase was 2.76 times greater since 1970 compared to the overall trend since 1900 (Fig. 4B), corresponding to the acceleration of climate change (Fig. 1). There was greater uncertainty in $\frac{\Delta\lambda}{\Delta Year}$ since 1970 because this estimate was based on fewer years. Under the trajectory since 1970, population growth is expected to reach the threshold of positive population growth ($\lambda = 1$) in the year 2057 (Fig. 4C); accelerating climate change would advance this transition to viable growth rates.

The stochastic population growth rate (λ_S), calculated over a sliding 10-year window, showed a similar trend of $\lambda_S < 1$ but increasing population growth rates over the past 120 years (Fig. C3). The stochastic growth rate reveals the effects of multi-year climate events, such as the runs of good years in the 1940s and 2000s.

Life Table Response Experiment

Life Table Response Experiments (LTRE) provided a decomposition of how λ responded to long-term climate trends (1900-2017), allowing us to understand the

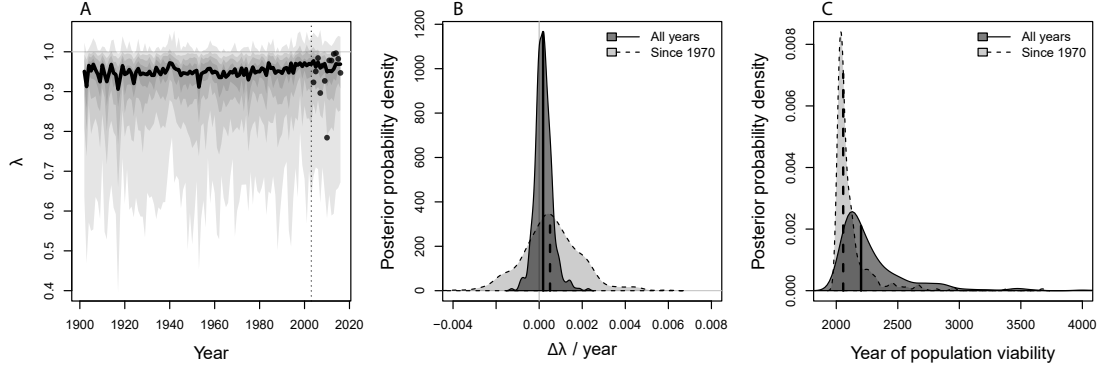


Figure 4: **A**, Posterior probability distribution for the time series of asymptotic population growth rates (λ) predicted based on inter-annual variation in three climate PCs. Thick black line shows the mean prediction and shaded regions show the 25, 50, 75, and 95% credible regions accounting for both parameter uncertainty and process error (year-to-year variation in vital rates that was unrelated to climate). Vertical line separates years that were back-casted versus years that were directly observed. The observation years (2004 and later) include estimates for year-specific population growth rates (points), captured statistically as year-specific random effects in the vital rates. **B**, Posterior distributions for the rate of temporal change in population growth ($\frac{\Delta\lambda}{\Delta Y_{\text{year}}}$). Dark grey shows the rate of change across all years shown in **A** and light grey shows the rate of change since 1970. Vertical lines show median values. **C**, Posterior distributions for the year of population viability ($\lambda = 1$) for the subset of posterior samples for which $\frac{\Delta\lambda}{\Delta Y_{\text{year}}} > 0$. Shading and lines as in **B**.

relative importance of different dimensions of climate variability and vital rate responses to them. LTRE results indicated that survival responses to climate were the overwhelming driver of temporal trends in λ (Fig. 5). Individual growth made no contribution to these trends because it was unresponsive to climate (Fig. D,E,F), whereas flowering and fertility were responsive to climate but their role was relatively small and imperceptible in Fig. 5. Furthermore, survival responses to climate PC2 were the dominant driver of temporal trends, followed by PC3 and then PC1. Collectively, responses to PC2 and PC3 accounted for 91% of the

381 overall climate effect in back-casted values of λ .

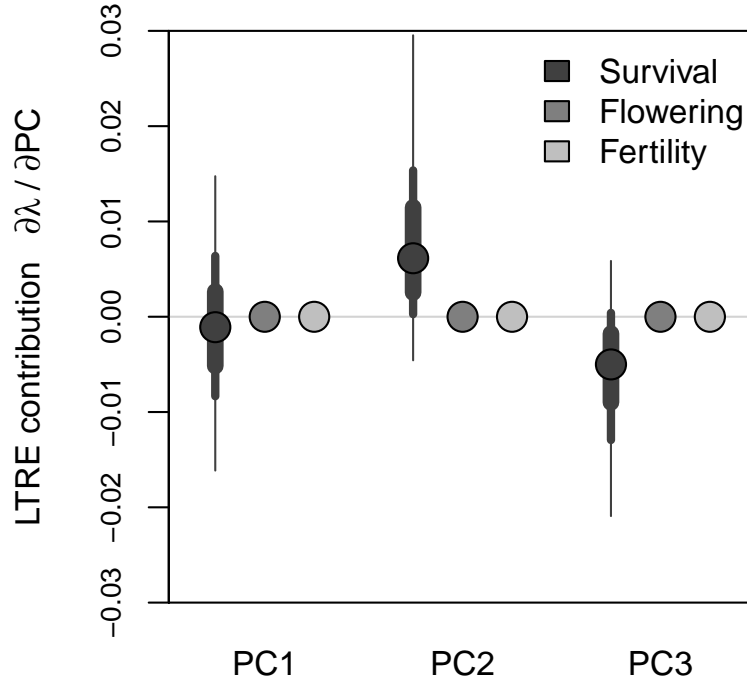


Figure 5: LTR decomposition of climate-driven inter-annual variability in population growth rates. Lines of decreasing thickness show the 50, 75 and 95 percentiles of the posterior distributions of the vital rate parameters, and points show the median. Shading corresponds to different vital rates (survival, flowering, and fertility) Posterior distributions for flowering and fertility are imperceptible on this scale.

Discussion

We began this work with the hypothesis that the apparent extinction debt of our study population was a consequence of recent climate change. Surprisingly, our results suggest the opposite: *C. imbricata* is likely a climate change “winner”, on an accelerating trajectory of increasing (less negative) population growth rates toward replacement-level within 38 years if current climate change trends persist, and sooner if they accelerate. We further show that the strongest feature of climate change in this system (the trend toward years that are overall warmer and drier, captured by PC1) was not the main driver of population responses. Instead, temporal trends in population viability were dominated by more subtle climatic factors with relatively weak signals of recent change (the trend toward wetter and milder cool seasons, captured by PCs 2 and 3). Our results highlight the challenges of forecasting population responses to climate change, since the strongest and therefore most detectable features of climate change may not be the most important drivers of ecological responses. At the same time, our work highlights how population biologists can meet this challenge through careful accounting of potentially diverse climate influences within a demographic modeling framework.

Our reconstruction of 120 years of population growth revealed a trajectory that was most likely positive, meaning that the climate has likely never been better for *C. imbricata* than it is now. This result begs the question of how these plants have reached their current, relatively high abundance, given over a century of population growth rates that were inferred to fall well below replacement levels. Land use history – which is not incorporated into our back-casted estimates – may have played a role. The Sevilleta NWR was exposed to grazing for much of

406 the 20th century until 1973. Previous work suggests that cacti, and *C. imbricata*
 407 in particular, can increase in abundance in response to grazing, due to livestock
 408 dispersing detached stem segment and thus promoting asexual regeneration (Allen
 409 *et al.*, 1991). During our study, we observed recruitment to be almost exclu-
 410 sively from seed (sexual and asexual recruits are easily distinguishable), though
 411 it is possible that regeneration dynamics were different under historical grazing
 412 regimes. Grazing may have also promoted cactus populations through release of
 413 competitive interactions with grasses (Yu *et al.*, 2019). Thus, one hypothesis is
 414 that *C. imbricata* achieved current densities under the historical land use regime,
 415 and cannot maintain these densities in the absence of cattle grazing. Given the
 416 potentially long lifespans of these plants, it may requires several decades more for
 417 the legacy of 20th-century land use to fade. An alternative hypothesis is that, inde-
 418 pendent of grazing or other land use history, our study population may be located
 419 in ‘sink’ habitat and maintained by dispersal from nearby populations that are
 420 more viable. Indeed, previous work showed that *C. imbricata* at lower elevations
 421 had positive population growth rates (Miller *et al.*, 2009) and may therefore act as
 422 source populations. Regardless of which process or processes best account for the
 423 persistence of a population that is currently inviable, our results indicate that it
 424 will likely be ‘rescued’ by ongoing climate change. One caveat to this conclusion
 425 is that, beyond the mean climate trends we have described, future climate (and
 426 especially monsoon precipitation) in our region is expected to be more variable
 427 (Rudgers *et al.*, 2018; Cook *et al.*, 2015) and this may dampen population growth
 428 independently of mean conditions (Boyce *et al.*, 2006). However, our stochastic
 429 demographic analysis, which accounts for increasing climate variability during the
 430 20th century, also showed a positive trajectory of λ_S (Fig. C3).

431 Until recently, few plant demographic studies explicitly considered climatic
 432 drivers of inter-annual variation (Ehrlén *et al.*, 2016; Crone *et al.*, 2011), though
 433 this is rapidly changing, especially as the GLM framework of IPMs very natu-
 434 rally incorporates abiotic covariates. To our knowledge, ours is the first study to
 435 compare the magnitudes of different aspects of climate change alongside the mag-
 436 nitudes of demographic responses to those changes. Consequently, further studies
 437 will be required to evaluate how commonly demographic responses are primarily
 438 driven by relatively weak components of climate change, as we found. However, we
 439 suspect that these patterns may be common since at the heart of our results lies the
 440 difference between annual versus seasonal climate trends. Specifically, we found
 441 that annual rainfall totals have been decreasing but that more of the annual rainfall
 442 has been falling in the cool season, consistent with previous climatological studies
 443 in our region that suggest a shift from warm- to cool-season precipitation (Cook &
 444 Seager, 2013; Cook *et al.*, 2015; Petrie *et al.*, 2014). Similarly, annual temperatures
 445 have been increasing in our study region but it was cool-season warming, specif-
 446 ically, that was most important for *C. imbricata* demography. Many plant and
 447 animal life histories operate on seasonal schedules and may therefore be more sen-
 448 sitive to seasonal redistribution of rainfall and temperature than to climate effects
 449 that manifest over an entire year, as we found for *C. imbricata*. Our results are
 450 consistent with previous studies that demonstrate the importance of considering
 451 seasonal, not annual, drivers of plant demographic responses (Selwood *et al.*, 2015;
 452 Williams *et al.*, 2015; Dahlgren *et al.*, 2016). Some recent studies have taken a
 453 finer-grained approach, connecting plant responses to weather events on monthly,
 454 weekly, or even daily time scales (Teller *et al.*, 2016; Tenhumberg *et al.*, 2018;
 455 Shriver, 2016). For tractability, we did not explore lagged climate effects beyond

one year, though methods for doing so are rapidly developing (Teller *et al.*, 2016; Tenhumberg *et al.*, 2018; Ogle *et al.*, 2015). Finding the appropriate timing and resolution of climate covariates will be an important area for future work as plant population biologists increasingly turn to environmentally explicit demographic models.

Rigorously accounting for various types of uncertainty will also be an important area in the development of environmentally explicit models for forecasting or back-casting. Even with strong climate-demography relationships detected with our unusually long-term data set, climate drivers accounted for little over half of the inter-annual variation in λ during the study years. It was therefore important to place our predictions for historical growth rates in the context of the substantial uncertainty that arose from process error: all the additional, unspecified ways that years may differ. We have emphasized the positive trajectory of population viability as the most likely trend in λ , but this should be interpreted in light of the probability distributions that we provide (Fig. 4) – that is, with nuance and appropriate caution¹. As ecologists are increasingly called upon to forecast responses to change in climate drivers, it will be essential to do so in a probabilistic framework that accommodates process error, i.e., the variability *not* explained by climate drivers.

Different aspects of a species' life cycle may respond in diverse ways to environmental drivers (Doak & Morris, 2010; Villellas *et al.*, 2015), highlighting the additional importance of considering multiple vital rates for understanding responses to global change. Our work was able to pinpoint which responses throughout the life

¹The odds that λ is increasing were slightly lower than the odds of a Clinton victory in the 2016 U.S. presidential election: <https://projects.fivethirtyeight.com/2016-election-forecast/>

cycle were most important for the overall population response to climate. Flower-
 ing and fertility were strongly sensitive to climate but the asymptotic population
 growth rate was very weakly sensitive to these reproductive processes, such that
 they made virtually no contribution to the overall population response to climate
 (Fig. 2, 5). On the other hand, survival responses to climate were relatively weak
 but λ was highly sensitive to small changes in survival, leading to strong population
 impacts. Vegetative growth, another high-sensitivity vital rate (Elder & Miller,
 2016), showed no significant responses to climate. These trends are consistent with
 previous findings that high-sensitivity vital rates (those that strongly influence λ)
 are buffered against environmental variability while low-sensitivity vital rates may
 exhibit wide fluctuations (Pfister, 1998). However, incomplete buffering of survival
 led to greater mortality in years with cold and dry cool-seasons – years that are be-
 coming less frequent under climate change (Fig. 1) – and these survival responses
 dominated the overall increase in population viability over the past 120 years
 (Fig. 5). These results mirror a recent study of another long-lived perennial plant,
 the alpine sunflower *Helianthella quinquinervis*, where reproductive responses to
 climate drivers were strong but ultimately overwhelmed by weaker responses in
 survival that more strongly affected population growth (Iler *et al.*, 2019). It is
 commonly observed that demographic transitions related to growth and survival
 are the most important determinants of population viability in species with long-
 lived perennial life histories (Franco & Silvertown, 2004). It may therefore be a
 general result that climate effects on growth and survival will be more consequen-
 tial in long-lived perennials than effects on reproductive processes, even as the
 latter exhibit greater sensitivity to climate, since perennials have many reproduc-
 tive opportunities over potentially long lifespans (Dalglish *et al.*, 2010; Morris

504 *et al.*, 2008).

505 Previous studies of cacti have emphasized their sensitivity to freezing as a con-
506 straint on physiological performance and geographic distribution (Flores & Yeaton,
507 2003; Kinraide, 1978; Nobel, 1984). In our study, we detected an important role
508 for winter minimum temperature and observed high mortality following record low
509 winter temperatures over a multi-day deep-freeze in 2011 (this is the low outlier in
510 Fig. 4A). As these freezing events become less frequent under climate change, we
511 expect an increase in regional abundance and perhaps northern expansion of *C.*
512 *imbricata*'s range, which currently extends to southern Colorado and is likely lim-
513 ited by winter minimum temperatures. This may be an issue of applied concern in
514 the region since *C. imbricata* is considered undesirable, particularly on rangelands
515 (Allen *et al.*, 1991). The role of cool-season precipitation that we detected was
516 more surprising. A majority of annual precipitation in the Southwest US comes
517 from warm-season monsoon events (Adams & Comrie, 1997) and these events
518 play a critical role in vegetation dynamics (Notaro & Gutzler, 2012; Petrie *et al.*,
519 2014), especially for plants with C4 and CAM photosynthesis that are physiologi-
520 cally most active during the warm summer months. Previous cactus demographic
521 studies have emphasized the role of summer monsoon precipitation (Winkler *et al.*,
522 2018; Bowers, 2005). Our results suggest that, despite its summer-adapted CAM
523 photosynthetic pathway, *C. imbricata* is able to capitalize on cool-season moisture,
524 and this was an important component of the positive demographic effects of recent
525 climate change. Predicting climate change winners and losers based on physiolog-
526 ical traits is a grand challenge in ecology. Our results raise new questions about
527 how well photosynthetic traits can predict responses to seasonal redistribution of
528 rainfall.

529 Several limitations of our study warrant consideration in the interpretation of
530 our results. First, our consideration of climate dependence was limited to four
531 vital rate processes of established plants. Because we could not reliably assign a
532 birth year to new recruits, we did not incorporate climate dependence in seedling
533 recruitment. Previous studies of cactus demography suggest that seedling recruit-
534 ment may be highly sensitive to climate, especially monsoon precipitation (e.g.,
535 Bowers 2005; Winkler *et al.* 2018). We suspect this is the case for *C. imbricata*,
536 since germination usually coincides with late-summer monsoons (*T.E.X. Miller*,
537 *unpubl. data*). Because we did not model this process as climate-dependent, our
538 results for climate effects on population growth are conservative. However, con-
539 sistent with expectations for long-lived perennials, we know seedling recruitment
540 to have very low eigenvalue sensitivities (Elder & Miller, 2016), which suggests
541 that even large climate effects on this process may not strongly register in terms
542 of population growth, as we observed for the reproductive functions of established
543 plants (Fig. 4B).

544 A second limitation to consider is that our approach to quantifying climate
545 drivers knowingly forfeits some information, and in two ways. First, in order to
546 gain deep temporal coverage, we relied on downscaled climate projections rather
547 than direct climatological observations. While we know these two types of data
548 to be highly correlated (Fig. A1), they are not perfectly so; this is especially true
549 for temperature minima and maxima (Table A1), where downscaled data likely
550 mis-estimate localized extremes. It is noteworthy that the downscaled climate
551 data poorly captured the extreme deep-freeze of winter 2011 (Fig. A1). Poor
552 demographic performance in this year was consequently attributed to a statistical
553 random effect (Fig. 4A), though this was almost certainly a true climate effect.

554 Second, we limited our consideration of climate drivers to the first three principal
555 components of inter-annual variation. While these three components explained a
556 large majority of the variation (Fig. 1A), we are disregarding some of the more
557 subtle dimensions of climate variability and change. Given our main finding that
558 the strongest features of climate change are not the main determinants of popu-
559 lation responses, these neglected dimensions may include important demographic
560 drivers. These two factors mean that our conclusions for climate-dependence err
561 on the conservative side.

562 Third, like any observational study, our conclusions rest on statistical associ-
563 ations between climate and demography. Further experimental work to test the
564 associations we detected would be valuable, especially since our back-casting anal-
565 ysis required that we extrapolate demographic responses to conditions that were
566 not observed during our 14-year study. We think the extrapolated predictions of
567 our statistical models are reasonable (Fig. 2) but we intentionally avoided fore-
568 casting our demographic model into the future because climate projections for
569 our region deviate substantially from observed conditions. We therefore lacked
570 confidence in our ability to quantitatively forecast population responses to future
571 climatic conditions, but experimental manipulations that mimic these conditions
572 could help bridge the gap to a rigorous process-based forecast.

573 To conclude, this study illustrates how long-term patterns of population vi-
574 ability can be reconstructed through climate-demography relationships observed
575 on relatively short time scales. This allowed us to evaluate the hypothesis that
576 recent climate change has driven *C. imbricata* in our region into extinction debt,
577 a hypothesis that we soundly reject. Instead, this species is most likely a cli-
578 mate change winner, largely due to its positive responses, especially in survival,

579 to recent and ongoing shifts in cool-season temperature and precipitation. Inter-
580 estingly, changes in cool-season climate were not the strongest features of climate
581 change, but they were nonetheless the most important determinants of population
582 responses. The more general lesson for global change biologists is that relatively
583 subtle dimensions of climate change may trigger strong ecological responses.

584 **Acknowledgements**

585 This study was supported by the Sevilleta LTER (NSF LTER awards 1440478,
586 1655499, and 1748133) and by NSF-DEB-1754468. We thank U.S Fish and Wildlife
587 Service staff (especially J. Erz) for facilitating research access to Sevilleta NWR.
588 We thank M. Evans and E. Schultz for helpful discussions on modeling climate-
589 demography relationships. Finally, we thank the many students and colleagues
590 have contributed to long-term data collection, especially M. Donald and B. Ochocki.

591 **Author contributions**

592 TEXM initiated and maintains the long-term study. KC collected and analyzed
593 data and prepared a manuscript draft. TEXM finalized text and analyses. Both
594 coauthors approve this submission.

595 **Data accessibility**

596 All of the code for our statistical and demographic modeling is available at **https:**
597 **//github.com/texmiller/cholla_climate_IPM** and raw data will be published

598 in parallel with this manuscript.

599 References

- 600 Ådahl E, Lundberg P, Jonzen N (2006) From climate change to population change:
601 the need to consider annual life cycles. *Global Change Biology*, **12**, 1627–1633.
- 602 Adams DK, Comrie AC (1997) The north american monsoon. *Bulletin of the*
603 *American Meteorological Society*, **78**, 2197–2214.
- 604 Adler PB, Byrne KM, Leiker J (2013) Can the past predict the future? experi-
605 mental tests of historically based population models. *Global change biology*, **19**,
606 1793–1803.
- 607 Allen L, Allen E, Kunst C, Sosebee R (1991) A diffusion model for dispersal of
608 opuntia imbricata (cholla) on rangeland. *The Journal of Ecology*, pp. 1123–1135.
- 609 Bowers JE (2005) Influence of climatic variability on local population dynamics of
610 a sonoran desert platyopuntia. *Journal of Arid Environments*, **61**, 193–210.
- 611 Boyce MS, Haridas CV, Lee CT, Group NSDW, *et al.* (2006) Demography in an
612 increasingly variable world. *Trends in Ecology & Evolution*, **21**, 141–148.
- 613 Buckley LB, Kingsolver JG (2012) The demographic impacts of shifts in climate
614 means and extremes on alpine butterflies. *Functional Ecology*, **26**, 969–977.
- 615 Bustamante E, Búrquez A (2008) Effects of plant size and weather on the flowering
616 phenology of the organ pipe cactus (*stenocereus thurberi*). *Annals of Botany*,
617 **102**, 1019–1030.

- 618 Caswell H (2001) *Matrix Population Models*. Sinauer Associates, Inc., Sunderland,
619 MA, 2 edn.
- 620 Compagnoni A, Bibian AJ, Ochocki BM, *et al.* (2016) The effect of demographic
621 correlations on the stochastic population dynamics of perennial plants. *Ecolog-
622 ical Monographs*, **86**, 480–494.
- 623 Cook B, Seager R (2013) The response of the north american monsoon to increased
624 greenhouse gas forcing. *Journal of Geophysical Research: Atmospheres*, **118**,
625 1690–1699.
- 626 Cook BI, Ault TR, Smerdon JE (2015) Unprecedented 21st century drought risk
627 in the american southwest and central plains. *Science Advances*, **1**, e1400082.
- 628 Cook C (1942) Insects and weather as they influence growth of cactus on the
629 central great plains. *Ecology*, **23**, 209–214.
- 630 Crone EE, Menges ES, Ellis MM, *et al.* (2011) How do plant ecologists use matrix
631 population models? *Ecology letters*, **14**, 1–8.
- 632 Dahlgren JP, Bengtsson K, Ehrlén J (2016) The demography of climate-driven and
633 density-regulated population dynamics in a perennial plant. *Ecology*.
- 634 Dalgleish HJ, Koons DN, Adler PB (2010) Can life-history traits predict the re-
635 sponse of forb populations to changes in climate variability? *Journal of Ecology*,
636 **98**, 209–217.
- 637 Dalgleish HJ, Koons DN, Hooten MB, Moffet CA, Adler PB (2011) Climate influ-
638 ences the demography of three dominant sagebrush steppe plants. *Ecology*, **92**,
639 75–85.

- 640 Daly C, Halbleib M, Smith JI, *et al.* (2008) Physiographically sensitive mapping
641 of climatological temperature and precipitation across the conterminous united
642 states. *International Journal of Climatology: a Journal of the Royal Meteorological Society*, **28**, 2031–2064.
- 644 Doak DF, Morris WF (2010) Demographic compensation and tipping points in
645 climate-induced range shifts. *Nature*, **467**, 959.
- 646 Drezner TD (2003) A test of the relationship between seasonal rainfall and saguaro
647 cacti branching patterns. *Ecography*, **26**, 393–404.
- 648 Drezner TD, Balling RC (2002) Climatic controls of saguaro (*Carnegiea gigantea*)
649 regeneration: a potential link with el niño. *Physical Geography*, **23**, 465–475.
- 650 Dullinger S, Gatttringer A, Thuiller W, *et al.* (2012) Extinction debt of high-
651 mountain plants under twenty-first-century climate change. *Nature Climate Change*, **2**, 619.
- 653 Dybala KE, Eadie JM, Gardali T, Seavy NE, Herzog MP (2013) Projecting de-
654 mographic responses to climate change: adult and juvenile survival respond
655 differently to direct and indirect effects of weather in a passerine population.
656 *Global Change Biology*, **19**, 2688–2697.
- 657 Ehrlén J, Morris WF (2015) Predicting changes in the distribution and abundance
658 of species under environmental change. *Ecology Letters*, **18**, 303–314.
- 659 Ehrlén J, Morris WF, von Euler T, Dahlgren JP (2016) Advancing environmentally
660 explicit structured population models of plants. *Journal of Ecology*, **104**, 292–
661 305.

- 662 Elderd BD, Miller TE (2016) Quantifying demographic uncertainty: Bayesian
663 methods for integral projection models. *Ecological Monographs*, **86**, 125–144.
- 664 Flores JL, Yeaton R (2003) The replacement of arborescent cactus species along a
665 climatic gradient in the southern chihuahuan desert: competitive hierarchies and
666 response to freezing temperatures. *Journal of arid environments*, **55**, 583–594.
- 667 Franco M, Silvertown J (2004) A comparative demography of plants based upon
668 elasticities of vital rates. *Ecology*, **85**, 531–538.
- 669 Franklin SB, Gibson DJ, Robertson PA, Pohlmann JT, Fralish JS (1995) Parallel
670 analysis: a method for determining significant principal components. *Journal of*
671 *Vegetation Science*, **6**, 99–106.
- 672 Frederiksen M, Daunt F, Harris MP, Wanless S (2008) The demographic impact
673 of extreme events: stochastic weather drives survival and population dynamics
674 in a long-lived seabird. *Journal of Animal Ecology*, **77**, 1020–1029.
- 675 George EI, McCulloch RE (1993) Variable selection via gibbs sampling. *Journal*
676 *of the American Statistical Association*, **88**, 881–889.
- 677 Hastings A, Abbott KC, Cuddington K, *et al.* (2018) Transient phenomena in
678 ecology. *Science*, **361**, eaat6412.
- 679 Hijmans RJ, Cameron SE, Parra JL, Jones PG, Jarvis A (2005) Very high reso-
680 lution interpolated climate surfaces for global land areas. *International Journal*
681 *of Climatology: A Journal of the Royal Meteorological Society*, **25**, 1965–1978.
- 682 Hooten MB, Hobbs N (2015) A guide to bayesian model selection for ecologists.
683 *Ecological Monographs*, **85**, 3–28.

684 Hultine K, Dettman D, Williams D, Puente R, English N, Butterfield B, Búrquez
 685 A (2018) Relationships among climate, stem growth, and biomass $\delta^{13}\text{C}$ in the
 686 giant saguaro cactus (*Carnegiea gigantea*). *Ecosphere*, **9**, e02498.

687 Hylander K, Ehrlén J (2013) The mechanisms causing extinction debts. *Trends in*
 688 *ecology & evolution*, **28**, 341–346.

689 Iler AM, Compagnoni A, Inouye DW, Williams JL, CaraDonna PJ, Anderson
 690 A, Miller TE (2019) Reproductive losses due to climate change-induced earlier
 691 flowering are not the primary threat to plant population viability in a perennial
 692 herb. *Journal of Ecology*, **107**, 1931–1943.

693 IPCC (2013) Contribution of working group I to the fifth assessment report of
 694 the intergovernmental panel on climate change. In: *Climate Change 2013: The*
 695 *Physical Science Basis*. (eds. Stocker TF, Qin D, Plattner GK, *et al.*). Cambridge
 696 University Press, Cambridge, United Kingdom and New York, NY, USA.

697 Jenouvrier S, Caswell H, Barbraud C, Holland M, Stroeve J, Weimerskirch H (2009)
 698 Demographic models and IPCC climate projections predict the decline of an em-
 699 peror penguin population. *Proceedings of the National Academy of Sciences*,
 700 **106**, 1844–1847.

701 Jenouvrier S, Holland M, Stroeve J, Serreze M, Barbraud C, Weimerskirch H,
 702 Caswell H (2014) Projected continent-wide declines of the emperor penguin un-
 703 der climate change. *Nature Climate Change*, **4**, 715.

704 Kinraide TB (1978) The ecological distribution of cholla cactus (*Opuntia imbricata*
 705 (Haw.) DC.) in El Paso County, Colorado. *The Southwestern Naturalist*, pp. 117–
 706 133.

- 707 Kuussaari M, Bommarco R, Heikkinen RK, *et al.* (2009) Extinction debt: a chal-
708 lenge for biodiversity conservation. *Trends in ecology & evolution*, **24**, 564–571.
- 709 Lehtilä K, Dahlgren JP, Garcia MB, Leimu R, Syrjänen K, Ehrlén J (2016) For-
710 est succession and population viability of grassland plants: long repayment of
711 extinction debt in *primula veris*. *Oecologia*, **181**, 125–135.
- 712 Lynch HJ, Rhainds M, Calabrese JM, Cantrell S, Cosner C, Fagan WF (2014) How
713 climate extremes—not means—define a species’ geographic range boundary via
714 a demographic tipping point. *Ecological Monographs*, **84**, 131–149.
- 715 Maschinski J, Baggs JE, QUINTANA-ASCENCIO PF, Menges ES (2006) Using
716 population viability analysis to predict the effects of climate change on the ex-
717 tinction risk of an endangered limestone endemic shrub, arizona cliffrose. *Con-*
718 *servation Biology*, **20**, 218–228.
- 719 McLean N, Lawson CR, Leech DI, van de Pol M (2016) Predicting when climate-
720 driven phenotypic change affects population dynamics. *Ecology Letters*, **19**,
721 595–608.
- 722 Miller TE, Louda SM, Rose KA, Eckberg JO (2009) Impacts of insect herbivory on
723 cactus population dynamics: experimental demography across an environmental
724 gradient. *Ecological Monographs*, **79**, 155–172.
- 725 Morris WF, Pfister CA, Tuljapurkar S, *et al.* (2008) Longevity can buffer plant and
726 animal populations against changing climatic variability. *Ecology*, **89**, 19–25.
- 727 Morrison SF, Hik DS (2007) Demographic analysis of a declining pika *ochotona*

728 collaris population: linking survival to broad-scale climate patterns via spring
729 snowmelt patterns. *Journal of Animal ecology*, **76**, 899–907.

730 Nobel PS (1984) Extreme temperatures and thermal tolerances for seedlings of
731 desert succulents. *Oecologia*, **62**, 310–317.

732 Notaro M, Gutzler D (2012) Simulated impact of vegetation on climate across the
733 north american monsoon region in ccs3. 5. *Climate dynamics*, **38**, 795–814.

734 Ogle K, Barber JJ, Barron-Gafford GA, *et al.* (2015) Quantifying ecological mem-
735 ory in plant and ecosystem processes. *Ecology letters*, **18**, 221–235.

736 Ohm JR, Miller TE (2014) Balancing anti-herbivore benefits and anti-pollinator
737 costs of defensive mutualists. *Ecology*, **95**, 2924–2935.

738 Parker KC (1993) Climatic effects on regeneration trends for two columnar cacti
739 in the northern sonoran desert. *Annals of the Association of American Geogra-*
740 *phers*, **83**, 452–474.

741 Peters DP, Havstad KM, Archer SR, Sala OE (2015) Beyond desertification: new
742 paradigms for dryland landscapes. *Frontiers in Ecology and the Environment*,
743 **13**, 4–12.

744 Petrie M, Collins S, Gutzler D, Moore D (2014) Regional trends and local variabil-
745 ity in monsoon precipitation in the northern chihuahuan desert, usa. *Journal of*
746 *arid environments*, **103**, 63–70.

747 Pfister CA (1998) Patterns of variance in stage-structured populations: evolution-
748 ary predictions and ecological implications. *Proceedings of the National Academy*
749 *of Sciences*, **95**, 213–218.

- 750 Plummer M, *et al.* (2003) Jags: A program for analysis of bayesian graphical
751 models using gibbs sampling. In: *Proceedings of the 3rd international workshop*
752 *on distributed statistical computing*, vol. 124. Vienna, Austria.
- 753 Reyes-García C, Andrade JL (2009) Crassulacean acid metabolism under global
754 climate change. *New Phytologist*, **181**, 754–757.
- 755 Rudgers JA, Chung YA, Maurer GE, Moore DI, Muldavin EH, Litvak ME, Collins
756 SL (2018) Climate sensitivity functions and net primary production: A frame-
757 work for incorporating climate mean and variability. *Ecology*, **99**, 576–582.
- 758 Selwood KE, McGeoch MA, Mac Nally R (2015) The effects of climate change
759 and land-use change on demographic rates and population viability. *Biological*
760 *Reviews*, **90**, 837–853.
- 761 Shriver RK (2016) Quantifying how short-term environmental variation leads to
762 long-term demographic responses to climate change. *Journal of Ecology*, **104**,
763 65–78.
- 764 Sletvold N, Dahlgren JP, Øien DI, Moen A, Ehrlén J (2013) Climate warming alters
765 effects of management on population viability of threatened species: results from
766 a 30-year experimental study on a rare orchid. *Global Change Biology*, **19**, 2729–
767 2738.
- 768 Smith M, Caswell H, Mettler-Cherry P (2005) Stochastic flood and precipitation
769 regimes and the population dynamics of a threatened floodplain plant. *Ecological*
770 *Applications*, **15**, 1036–1052.

771 Su YS, Yajima M (2012) R2jags: A package for running jags from r. *R package*
772 *version 0.03-08*, URL <http://CRAN.R-project.org/package=R2jags>.

773 Teller BJ, Adler PB, Edwards CB, Hooker G, Ellner SP (2016) Linking demogra-
774 phy with drivers: climate and competition. *Methods in Ecology and Evolution*,
775 **7**, 171–183.

776 Tenhumberg B, Crone EE, Ramula S, Tyre AJ (2018) Time-lagged effects of
777 weather on plant demography: drought and astragalus scaphoides. *Ecology*,
778 **99**, 915–925.

779 Urban MC (2015) Accelerating extinction risk from climate change. *Science*, **348**,
780 571–573.

781 Van de Pol M, Vindenes Y, Sæther BE, Engen S, Ens BJ, Oosterbeek K, Tinbergen
782 JM (2010) Effects of climate change and variability on population dynamics in
783 a long-lived shorebird. *Ecology*, **91**, 1192–1204.

784 Vellend M, Verheyen K, Jacquemyn H, Kolb A, Van Calster H, Peterken G, Hermy
785 M (2006) Extinction debt of forest plants persists for more than a century fol-
786 lowing habitat fragmentation. *Ecology*, **87**, 542–548.

787 Villellas J, Doak DF, García MB, Morris WF (2015) Demographic compensation
788 among populations: what is it, how does it arise and what are its implications?
789 *Ecology letters*, **18**, 1139–1152.

790 Wang T, Hamann A, Spittlehouse D, Carroll C (2016) Locally downscaled and
791 spatially customizable climate data for historical and future periods for north
792 america. *PLoS One*, **11**, e0156720.

- 793 Williams JL, Jacquemyn H, Ochocki BM, Brys R, Miller TE (2015) Life history
794 evolution under climate change and its influence on the population dynamics of
795 a long-lived plant. *Journal of Ecology*, **103**, 798–808.
- 796 Williams JL, Miller TEX, Ellner SP (2012) Avoiding unintentional eviction from
797 integral projection models. *Ecology*, **93**, 2008–2014.
- 798 Winkler DE, Conner JL, Huxman TE, Swann DE (2018) The interaction of drought
799 and habitat explain space–time patterns of establishment in saguaro (*Carnegiea*
800 *gigantea*). *Ecology*, **99**, 621–631.
- 801 Yu K, D’Odorico P, Collins SL, *et al.* (2019) The competitive advantage of a con-
802 stitutive CAM species over a C4 grass species under drought and CO2 enrichment.
803 *Ecosphere*, **10**, e02721.

804 Appendix A: Correspondence between downscaled 805 and locally measured climate variables

806 We compared warm- and cool-season values of four climate variables (total pre-
807 cipitation and minimum, mean, and maximum temperature) between two data
808 sources: the SEV-LTER meteorological station nearest our study site (station 50 in
809 the SEV-LTER meteorological network) and downscaled data from ClimateWNA
810 corresponding to the same latitude, longitude, and elevation as station 50. Our
811 goal was to determine how well the downscaled data captured conditions ‘on the
812 ground’ as measured directly by the meteorological station. We compared the
813 years 2001 through 2017, which are the years of overlap between the two data
814 sources.

815 There was generally strong agreement between the two data sources (Table A1,
816 Figure A1). Temperature extrema were less strongly correlated between the two
817 data sets than temperature means, which is unsurprising given that extreme values
818 may be sensitive to local micro-environmental conditions that the relatively coarse
819 downscaled data would miss. The weakest correlation was that of warm-season
820 maximum temperature (Spearman’s $r = 0.41$, $P = 0.11$).

Table A1: Correlations between seasonal climate values measured by an on-site meteorological station versus downscaled data from ClimateWNA corresponding to the same years and location. Correlation values show Pearson correlations and P-values come from t -tests with 14 degrees of freedom.

Season	Variable	Correlation	P-value
Warm	Min temperature	0.59	0.0153
Warm	Mean temperature	0.84	10^{-4}
Warm	Max temperature	0.41	0.1135
Warm	Precipitation	0.49	0.0544
Cool	Min temperature	0.51	0.0622
Cool	Mean temperature	0.94	3.6×10^{-7}
Cool	Max temperature	0.69	0.0069
Cool	Precipitation	0.87	4.6×10^{-5}

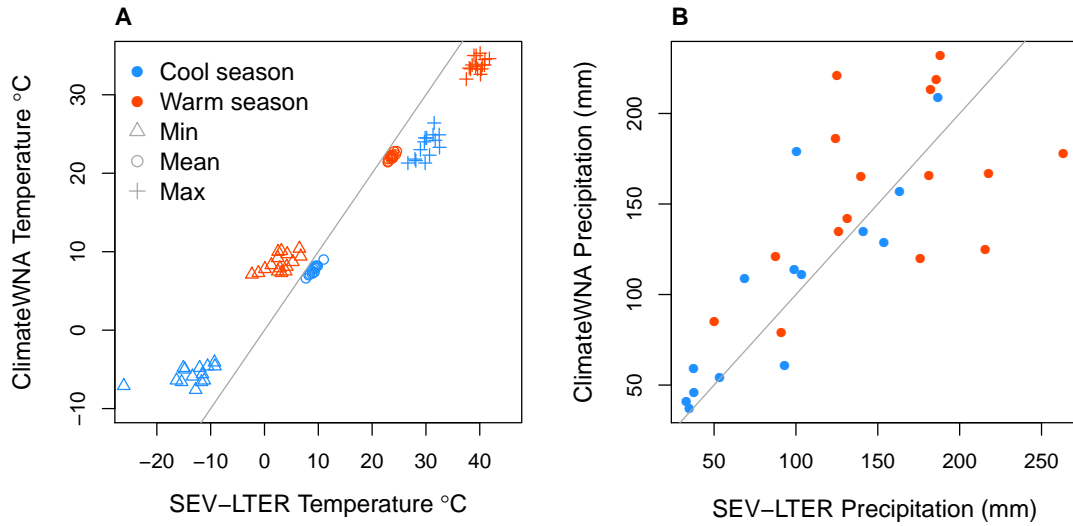


Figure A1: Correlations between seasonal climate values (**A**: temperature; **B**: precipitation) between SEV-LTER meteorological data and downscaled estimates from ClimateWNA for years 2001–2017. Gray lines show $y = x$.

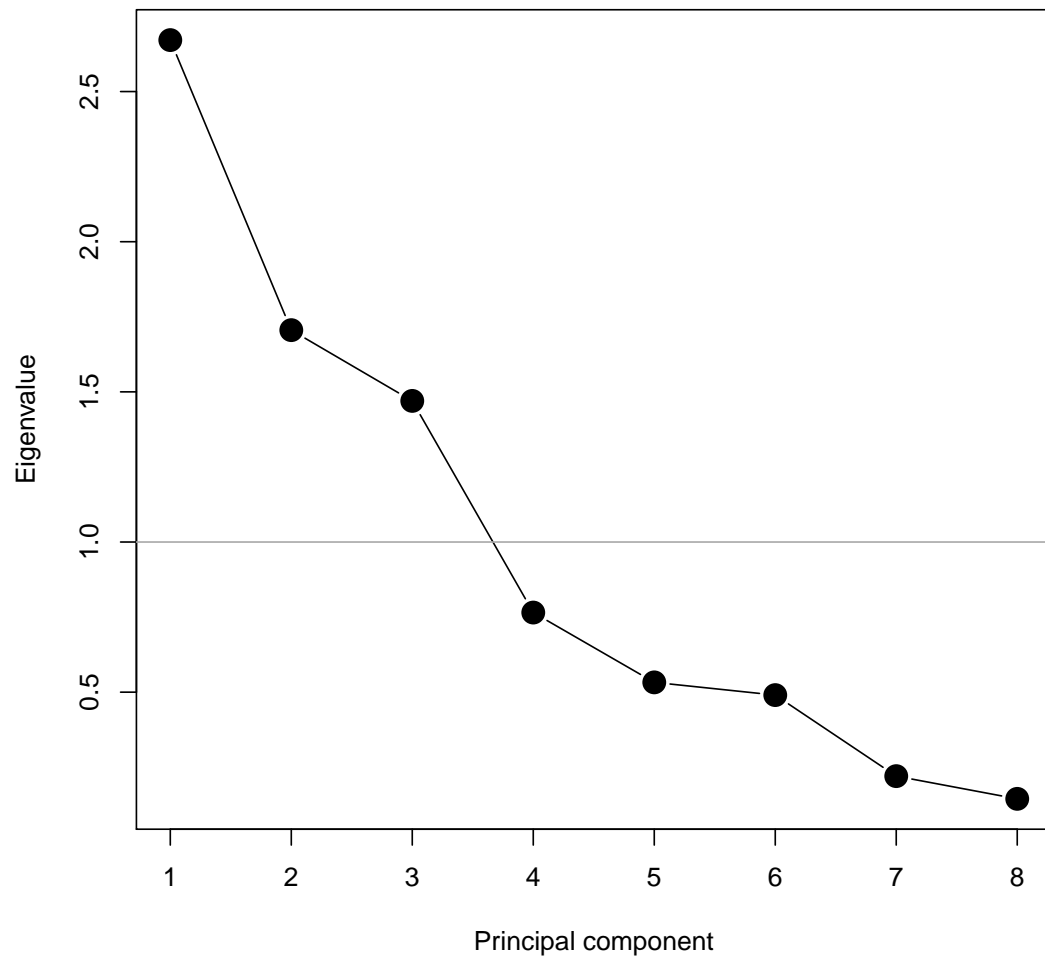


Figure A2: Parallel analysis.

821 Appendix B: Vital rate modeling and stochastic vari- 822 able selection

823 We fit generalized linear mixed effects models in a hierarchical Bayesian statisti-
824 cal framework to quantify climate dependence in demographic vital rates. There
825 were four size-dependent vital rates measured in the long-term study for which
826 we could additionally estimate climate dependence: survival from year t to year
827 $t+1$, individual growth (change in size from year t to year $t+1$), probability of
828 flowering in year t , and the number of flowerbuds produced year in t , given that a
829 plant flowered. All of the vital rate models used the same general linear predictor
830 for the expected value (μ) but apply a different link function ($f(\mu)$) depending on
831 the distribution of the observations:

$$\begin{aligned}
 f(\mu) = & \beta_0 + \beta_1 x + \\
 & \rho_1^1 PC1 + \rho_2^1 PC1^2 + \rho_3^1 x PC1 + \\
 & \rho_1^2 PC2 + \rho_2^2 PC2^2 + \rho_3^2 x PC2 + \\
 & \rho_1^3 PC3 + \rho_2^3 PC3^2 + \rho_3^3 x PC3 + \\
 & \gamma + \tau
 \end{aligned} \tag{B1}$$

832 The linear predictor includes a grand mean intercept (β_0) and size-dependent
833 slope (β_1). The size variable x is the natural logarithm of plant volume ($\log_e(cm^3)$),
834 which was standardized to mean zero and unit variance for analysis. Other fixed-
835 effect coefficients (ρ) correspond to climate variables and climate \times size inter-
836 actions. The climate variables are the three principal components ($PC1$, $PC2$,

837 *PC3*) of inter-annual variation in temperature and precipitation. We include
838 quadratic terms for climate to account for the possibility of non-monotonic cli-
839 mate responses. Climate coefficient (ρ) superscripts correspond to each PC, and
840 subscripts correspond to linear, quadratic, and size-interaction effects. Finally,
841 the linear predictor includes normally distributed random effects for plot-to-plot
842 variation ($\gamma \sim N(0, \sigma_{plot})$) and year-to-year variation that is unrelated to climate
843 effects captured by PCs 1-3 ($\alpha \sim N(0, \sigma_{year})$).

844 The growth data were normally distributed; this model applied the identity
845 link and included an additional parameter for residual variance. We explored size-
846 dependence in the residual variance of growth (which determines how individuals
847 are distributed around their expected future size) but found that this led to poorer
848 model fits, so we proceeded to assume a constant value. The survival and flower-
849 ing data were Bernoulli distributed, and these models applied the logit link func-
850 tion. The fertility data (flowerbud counts) were modeled as Poisson-distributed,
851 including an individual-level random effect to account for overdispersion. All co-
852 efficients were given vague priors. We evaluated model fits using posterior predic-
853 tive checks (Elder & Miller, 2016). All models were fit using JAGS (Plummer
854 *et al.*, 2003) and R2JAGS (Su & Yajima, 2012). Analysis code is available at
855 https://github.com/texmiller/cholla_climate_IPM.

856 Stochastic variable selection

857 Because we intended to extrapolate the vital rate models into past climate environ-
858 ments that were not well represented during the long-term study, it was important
859 that we simplify the vital rate models to exclude unnecessary coefficients (which,

860 even if small in absolute value, could generate unrealistic predictions when ex-
 861 trapolated over a greater range of climate than the models were fitted to). To
 862 do this, we used stochastic variable selection, a ‘model-based model selection’
 863 approach (Hooten & Hobbs, 2015) that generates weightings for each fixed-effect
 864 coefficient, indicating the probability that the coefficient is non-zero. We employed
 865 an approach based on George and McCulloch (1993) where each coefficient (C_i)
 866 is modeled as a mixture distribution with zero and non-zero modes, where modal
 867 frequency is determined by an indicator variable (z_i). The coefficient prior was:

$$C_i \sim (1 - z_i) * N(0, 0.1) + z_i * N(0, 1000) \quad (\text{B2})$$

$$z_i \sim \text{Bernoulli}(0.5) \quad (\text{B3})$$

868 The first term of the mixture distribution assigns, with probability $(1 - z_i)$, a
 869 prior with mean zero and arbitrarily small variance, effectively forcing the poste-
 870 rior estimate to equal zero. The second term assigns, with probability z_i , a prior
 871 with mean zero and arbitrarily large variance, which allows for a non-zero pos-
 872 terior estimate. The posterior distribution of the indicator variable z_i gives the
 873 probability that the coefficient is non-zero. We estimated this probability for each
 874 coefficient in Eq. B2 and retained in the final model all coefficients with a posterior
 875 mean $\hat{z}_i > 0.1$, meaning that the model term is determined to be non-zero with
 876 90% confidence. All z_i values from the full model are shown in Table B1.

Climate PC	Model term	Survival	Growth	Flowering	Fertility
	Size	1	0.53	1	1
1	PC	0.13	0.04	0.12	0.05
1	PC*PC	0.03	0.01	0.03	0.01
1	PC*size	0.06	0.01	0.08	0.07
2	PC	0.18	0.03	0.11	0.14
2	PC*PC	0.06	0.01	0.06	0.03
2	PC*size	0.04	0.02	1	0.27
3	PC	0.18	0.02	0.12	0.18
3	PC*PC	0.09	0.01	0.09	0.06
3	PC*size	0.06	0.01	0.13	0.03

Table B1: Stochastic variable selection results. Values (z) can be interpreted as the probability that a model coefficient is non-zero. Bolded values indicate terms retained in the final model.

877 Appendix C: Methods for IPM construction and 878 analysis

879 Model overview

880 The statistical models described in Appendix B formed the backbone of the inter-
881 gral projection model (IPM) that we used to estimate population growth in variable
882 climate environments. Figure C1 illustrates the timing of our demographic census
883 (a pre-breeding census) and climate events as they relate to the tree cholla life
884 cycle.

885 Following previous studies (Compagnoni *et al.*, 2016; Ohm & Miller, 2014;
886 Elderder & Miller, 2016), we modeled the life cycle of *C. imbricata* using contin-
887 uously size-structured plants, $n(x)$, and two discrete seed banks ($B_{1,t}$ and $B_{2,t}$)
888 corresponding to 1 and 2-year old seeds:

$$B_{1,t+1} = \kappa \delta \int_L^U P(x, \mathbf{c}_{t-1}; \alpha_t^P) F(x, \mathbf{c}_{t-1}; \alpha_t^F) n(x)_t dx \quad (\text{C1})$$

$$B_{2,t+1} = (1 - \gamma_1 B_{1,t}) \quad (\text{C2})$$

Functions P and F give the probability of flowering and the number of flower-
 buds produced, respectively, for an x -sized plant. The vector \mathbf{c}_{t-1} contains the
 climate PC values for climate-year $t - 1$, which affects flowering and fertility in
 year t , and hence the 1-year old seed bank in year $t + 1$. Parameters α_t^P and
 α_t^F are random year effects estimated from the statistical models. The integral
 is multiplied by the number of seeds per fruit (κ) and probability of seed disper-
 sal/survival (δ) to give the number of seeds that enter the 1-year old seed bank.
 The integral is evaluated from the lower (L) to upper (U) bounds of the plant size
 distribution. Plants can recruit out of the 1-year old seed bank with probability
 γ_1 or transition to the 2-year old seed bank with probability $(1 - \gamma_1)$. Seeds in the
 2-year old seed bank are assumed to either germinate (probability γ_2) or die.

Continuous-size dynamics are given by:

$$n(y)_{t+1} = (\gamma_1 B_{1,t} + \gamma_2 B_{2,t}) \eta(y) \omega + \int_L^U S(x, \mathbf{c}_t; \alpha_t^S) G(y, x, \mathbf{c}_t; \alpha_t^G) n(x)_t dx \quad (\text{C3})$$

The first term indicates recruitment from the seed banks to size y , where $\eta(y)$
 gives the seedling size distribution, assumed normal with mean μ_s and standard
 deviation σ_s . Mortality between germination (late summer) and the yearly demo-
 graphic census (May) is accounted for with survival probability ω . In the second
 term, functions S and G give the probabilities of surviving to year $t + 1$ and grow-

ing to size y , respectively, for an x -sized plant in year t . Climate-dependence and random year effects are included as in Eq. C1, except the timing of climate effects is shifted such that growth and survival from t to $t + 1$ are affected by climate over the same interval. As above, survival and growth functions also take time-varying random intercepts.

Equations C1 – C3 clearly show where in the life cycle we include climate effects and where we do not. All climate-independent processes (primarily related to seed banks and seedling recruitment) were parameterized from field data. These methods are described elsewhere (Compagnoni *et al.*, 2016; Elderd & Miller, 2016). All parameter estimates are provided in Table C1.

Model analysis

Following our statistical models, the size variable x was the natural logarithm of plant volume ($\log_e(\text{cm}^3)$). For analysis, we discretize x into n bins, replacing the continuous kernel with an n -by- n matrix (because our model also included two additional discrete states, the final projection matrix had dimensions $n + 2$ -by- $n + 2$). We used $n = 200$ bins. We extended integration limits L and U to avoid unintentional “eviction” (Williams *et al.*, 2012).

We estimated the asymptotic population growth rate λ as the dominant eigenvalue of the discretized IPM kernel. We compared the observed size distribution and the predicted distribution at the long-term mean climate ($PC_1 = PC_2 = PC_3 = 0$). These generally corresponded well (Fig. C2), though very large plants were over-represented in the observed size distribution. This is consistent with the idea that the population may have recently transitioned into decline, whereby the

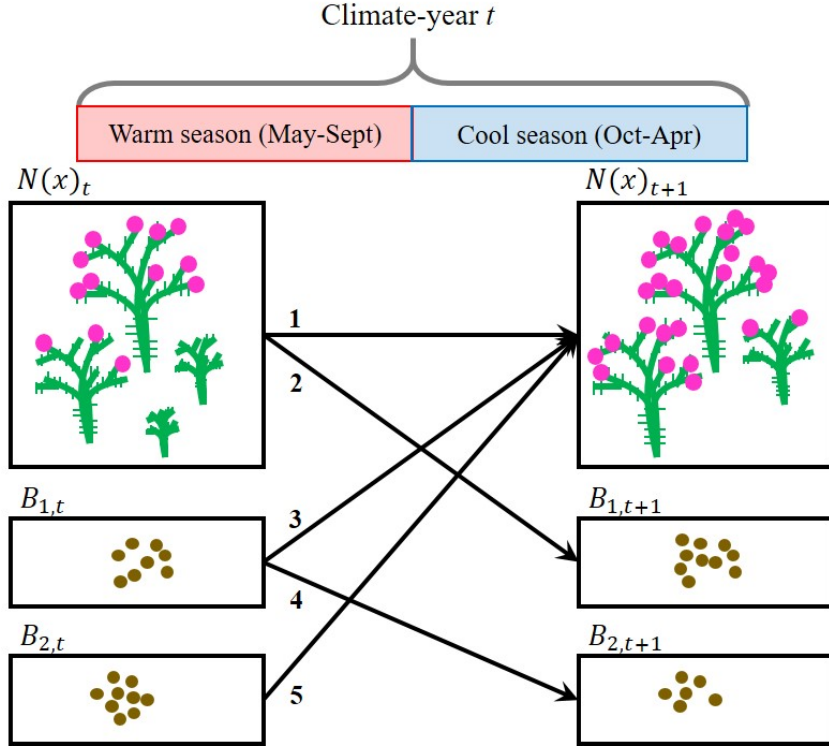


Figure C1: *C. imbricata* life cycle and census timing with respect to warm- and cool-season climate. Numbered arrows correspond to demographic events that occur during a transition year: (1) established plants survive and grow, (2) plants that are reproductive in year t contribute seeds that will make up the 1-yo seed bank in year $t+1$, (3) a fraction of seeds in the 1-yo seed bank survive and recruit into the plant population as seedlings in year $t+1$, (4) another fraction of seeds in the 1-yo seed bank survives and remains to form the 2-yo seed bank in year $t+1$, (5) a fraction of seeds in the 2-yo seed bank survive and recruit into the plant population as seedlings in year $t+1$. Survival and growth from year t to year $t+1$ (arrow 1) depended on climate year year t , whereas flowering and flowerbud production in year t (components of arrow 2) depended on climate in year $t-1$.

928 persistence of large plants may reflect a legacy of positive growth rates. Also, the
 929 left peak for new recruits was at a larger size in the observed distribution, but
 930 this was likely a consequence of the fact that we rarely detected new recruits. The
 931 smallest plants in our census were likely several years old.

932 We evaluated how λ responded to climate variation by first varying each climate
 933 PC independently, holding the other two fixed at their long-term mean. Second, we
 934 back-casted λ over the 20th century using time series of PC values, which generated
 935 a time series of λ_t .

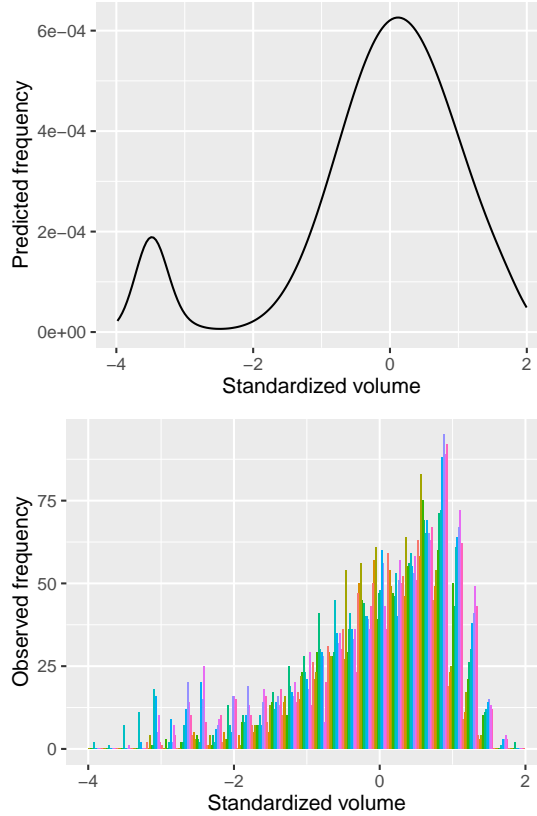


Figure C2: Comparison of predicted (top) and observed (bottom) size distributions, where size was the natural logarithm of plant volume standardized to mean zero. In the bottom panel, different colors represent different years.

936 Life Table Response Experiment

We used Life Table Response Experiments (LTREs) to decompose which combinations of climate PCs and vital rate responses were most strongly responsible for

temporal fluctuations in the back-casted time series λ_t . We used a fixed-design LTRE (Caswell, 2001) where λ_t was defined as a linear function of climate predictors:

$$\lambda_t = \bar{\lambda} + \sum_{i=1}^3 \beta_i PC_i \quad (\text{C4})$$

There is no error term because, in this analysis, climate PCs are assumed to be the sole drivers of fluctuations in λ_t . The coefficient for each climate PC was approximated as:

$$\beta_i \approx \sum_{j=1}^n \frac{\partial \bar{\lambda}}{\partial \theta_j} \frac{\partial \theta_j}{\partial PC_i} \quad (\text{C5})$$

937 The LTRE approximation is based on the product of the sensitivity of λ to the vital
 938 rates (θ), evaluated at the long-term mean climate ($PC_1 = PC_2 = PC_3 = 0$), and
 939 the sensitivity of the vital rates to climate, summed over all vital rates n . Because
 940 LTRE components are additive, we summed LTRE estimates over the intercept
 941 and slope of each vital rate function so that we could interpret the results in terms
 942 of vital rate contributions. We verified that the LTRE approximations matched
 943 the Maximum Likelihood estimates for Eq. C4.

944 Stochastic population growth

We simulated population dynamics according to Equations C3–C1 to estimate the stochastic population growth rate λ_S . λ_S represents the expected long-term growth rate in a variable environment, accounting for vital rate fluctuations and temporal auto-correlation in environmental drivers. We estimated λ_S for 10-year

windows spanning the time series 1901–2017, such that the value of λ_S for year t reflects the stochastic growth rate for a climate environment defined by years t through $t + 9$. For each 10-year window, we simulated 1000 years of population dynamics, each year randomly drawing one of the 10 climate-years. For each year of the simulation, we calculated total population size as:

$$N_t = \int n(x)_t dx + B_{1,t} + B_{2,t} \quad (\text{C6})$$

and estimated the stochastic growth rate for that window as the expected value of the one-year growth rate:

$$\log(\lambda_S) = \mathbb{E}[\log(\frac{N_{t+1}}{N_t})] \quad (\text{C7})$$

Table C1: Parameter values of tree cholla IPM.

Parameter description	Symbol	Mean	95%CI
Survival coefficients	β_0	3.33	(1.4 – 5.25)
	β_1	1.31	(1.18 – 1.44)
	ρ_1^1	-0.11	(-0.82 – 0.61)
	ρ_1^2	0.41	(-0.25 – 1.13)
	ρ_1^3	-0.28	(-0.84 – 0.3)
Growth coefficients	β_0	-0.03	(-0.08 – 0.02)
	β_1	-0.02	(-0.03 – -0.02)
Growth standard deviation	σ	0.25	(0.25 – 0.26)
Flowering coefficients	β_0	-4.76	(-7.37 – -2.22)
	β_1	5.17	(4.78 – 5.54)
	ρ_1^1	-0.26	(-1.27 – 0.7)
	ρ_1^2	0.07	(-0.85 – 1.01)
	ρ_3^2	1.11	(0.65 – 1.61)
	ρ_1^3	-0.04	(-0.79 – 0.77)
	ρ_3^3	0.21	(-0.06 – 0.47)
Fertility coefficients	β_0	-0.25	(-0.6 – 0.1)
	β_1	2.22	(2.01 – 2.42)
	ρ_1^2	0.06	(-0.15 – 0.28)
	ρ_3^2	0.17	(-0.01 – 0.35)
	ρ_1^3	0.12	(-0.04 – 0.29)
Seeds per fruit	κ	113.46	(93.47 – 132.59)
Recruitment into seed bank	δ	0.03	(0.02 – 0.05)
Germination rates	γ_1	0.0059	(0.0047 – 0.0073)
	γ_2	0.0044	(0.0033 – 0.0056)
Seedling size distribution	μ_s	-3.49	(-3.62 – -3.37)
	σ_s	0.23	(0.15 – 0.35)
Seedling survival	ω	0.5	(0.002 – 0.998)
Size bounds	L	-3.94	
	U	1.89	

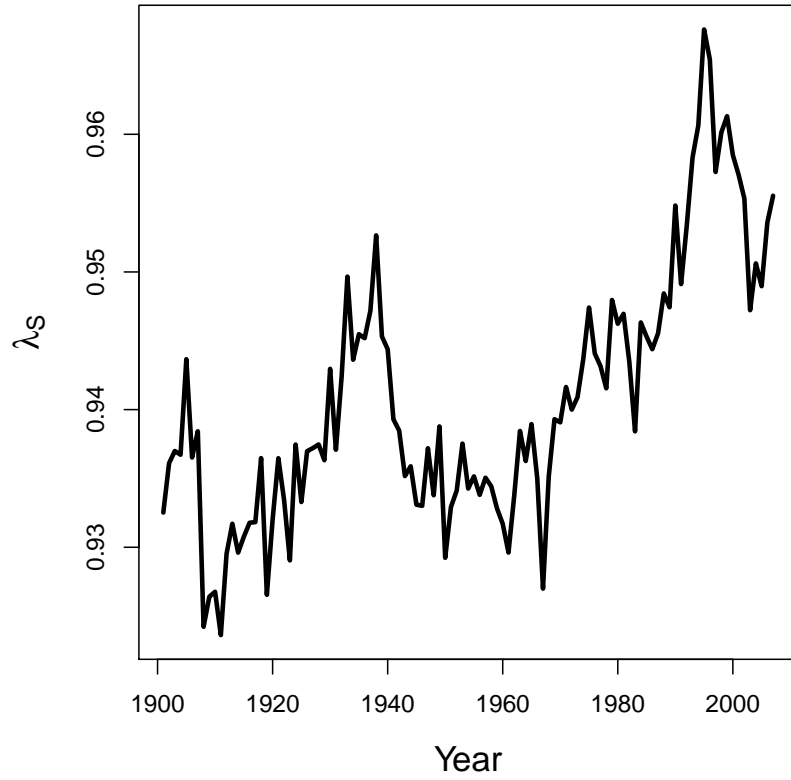


Figure C3: Time series of stochastic population growth rates (λ_S). Values are based on a 10-year sliding window such that λ_S is year t is based on the climate regime over the years t through $t + 9$